

Figure 1: A schematic displaying the effect of configurational entropy on the stabilization of single-phase solid solution around the equiatomic composition, where  $x_i$  is the molar fraction of component  $i$ ,  $n$  the number of components in equiatomic proportion,  $G$  the Gibbs free energy of a phase  $t$  ( ${}^{ref}$ ,  ${}^{cnf}$  and  ${}^E$  stand for reference, configurational and excess, respectively). In the resulting ternary system calculated from the association of three binaries with a miscibility gap, single solid solution phases are displayed in blue, while green and white denote binary and ternary phase fields.  $\Delta h^{im}$  represents the enthalpy of formation of intermetallic compounds. According [4], 50% of intermetallics have  $\Delta h^{im}$  above 10 kJ/mol. It appears that configurational entropy can compete with enthalpy at high temperature. Finally, the distinguishing feature of the alloying concept behind HEAs and CCAs that is the exploration of the vast interior region of the composition space is illustrated in contrast with the classical design strategy that focuses on the peripheral regions of phase diagrams.

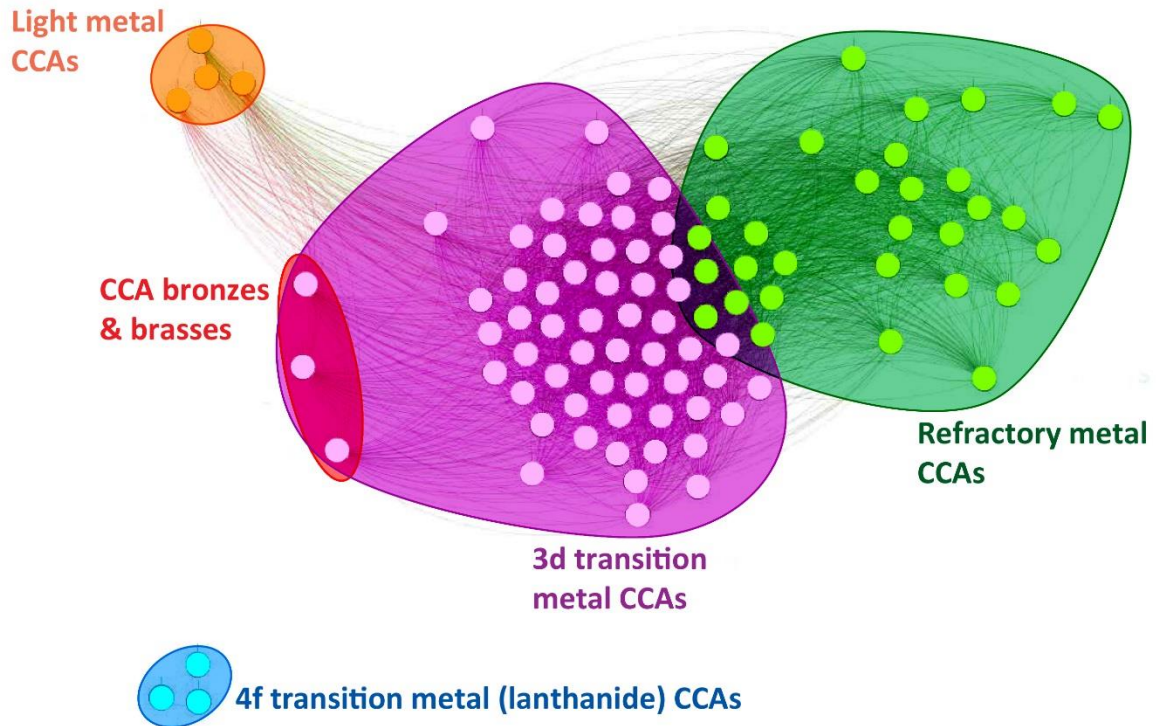


Figure 2: Alloy network analysis (ANA) of 110 equiatomic CCAs. Each node is a unique alloy and a line connecting two nodes indicates sharing of one or more common element. Nodes (alloys) that often share many elements are spaced closely together into specific alloy families. See text for additional description of this plotting method.

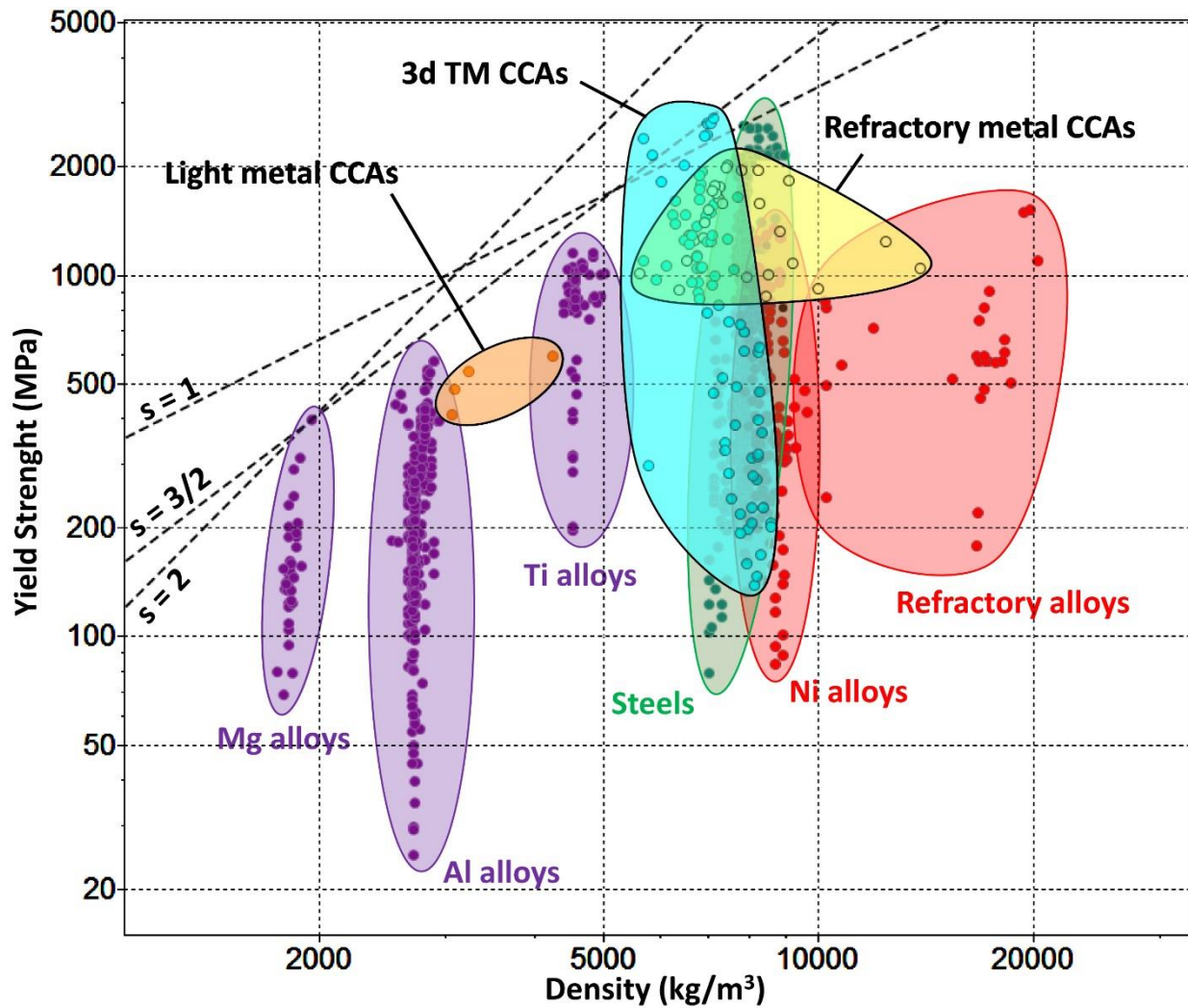
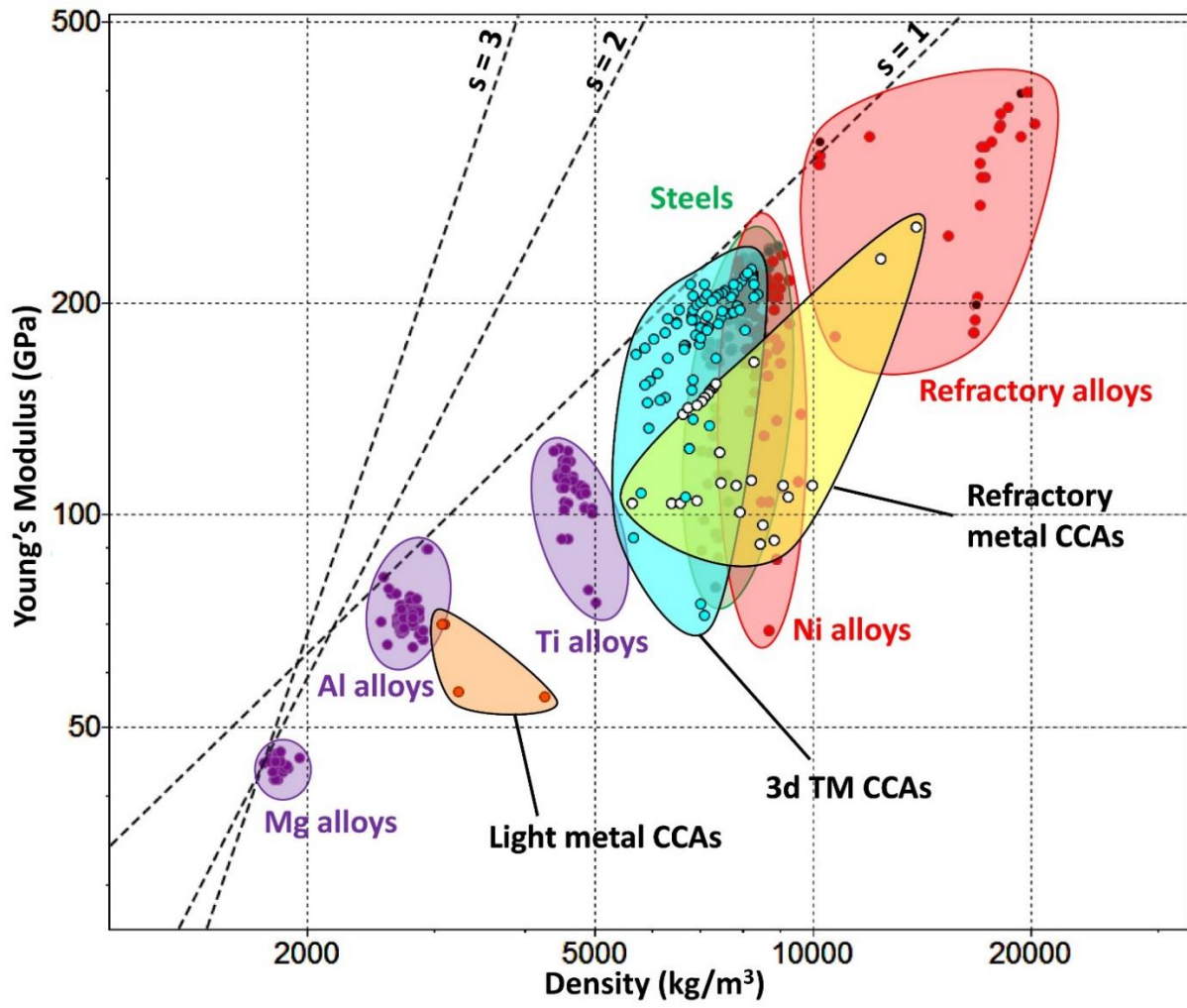
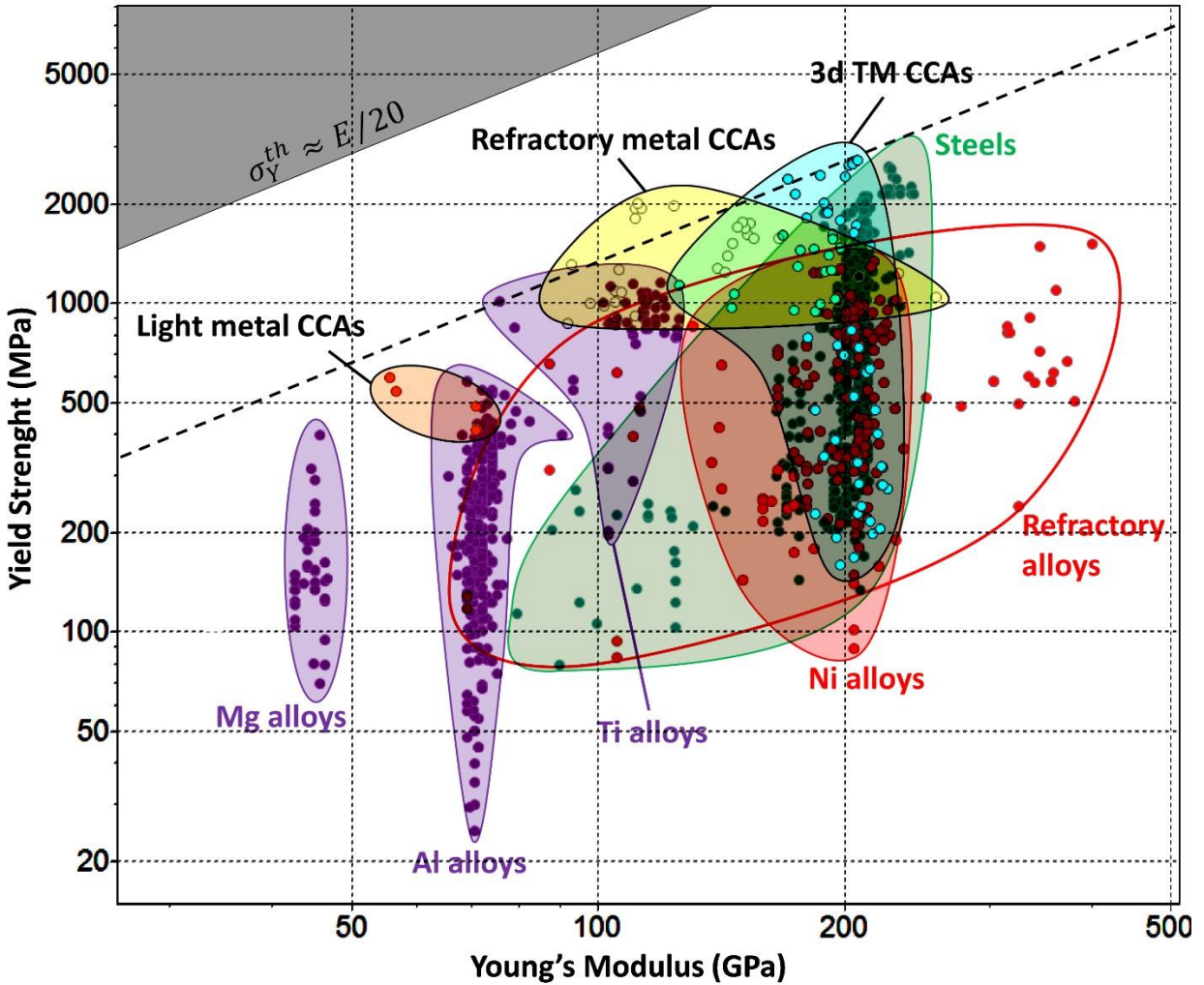


Figure 3: Materials property space for room temperature yield strength vs density of conventional metal alloys and CCAs. 3d transition metal CCAs are shown by teal-colored bubbles, refractory metal CCAs are shown by yellow bubbles and light metal CCAs are shown by orange bubbles. The dashed lines give performance indices for uniaxial loading (slope,  $s = 1$ ), beam bending ( $s = 3/2$ ) and panel bending ( $s = 2$ ). See the text for additional discussion of this plot. This chart was made with the CES EduPack database, Level 3 Aerospace edition and the CCA database from the present work. It displays data for about 1220 commercial and 120 multi-principle element alloys.

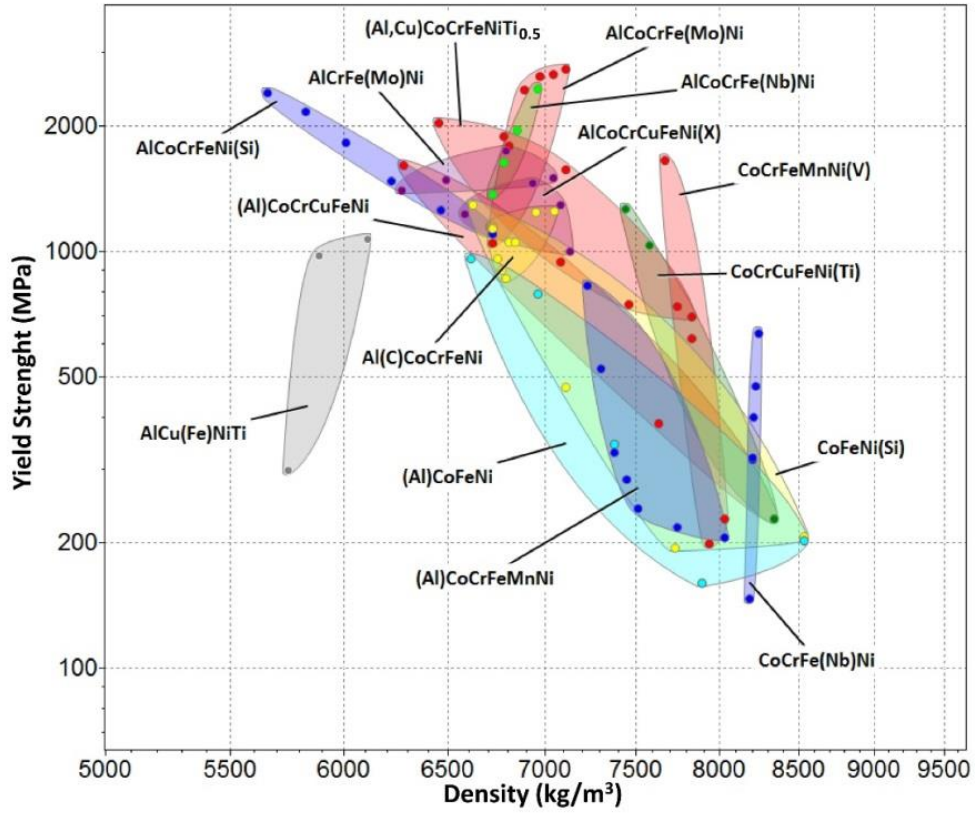


(a)

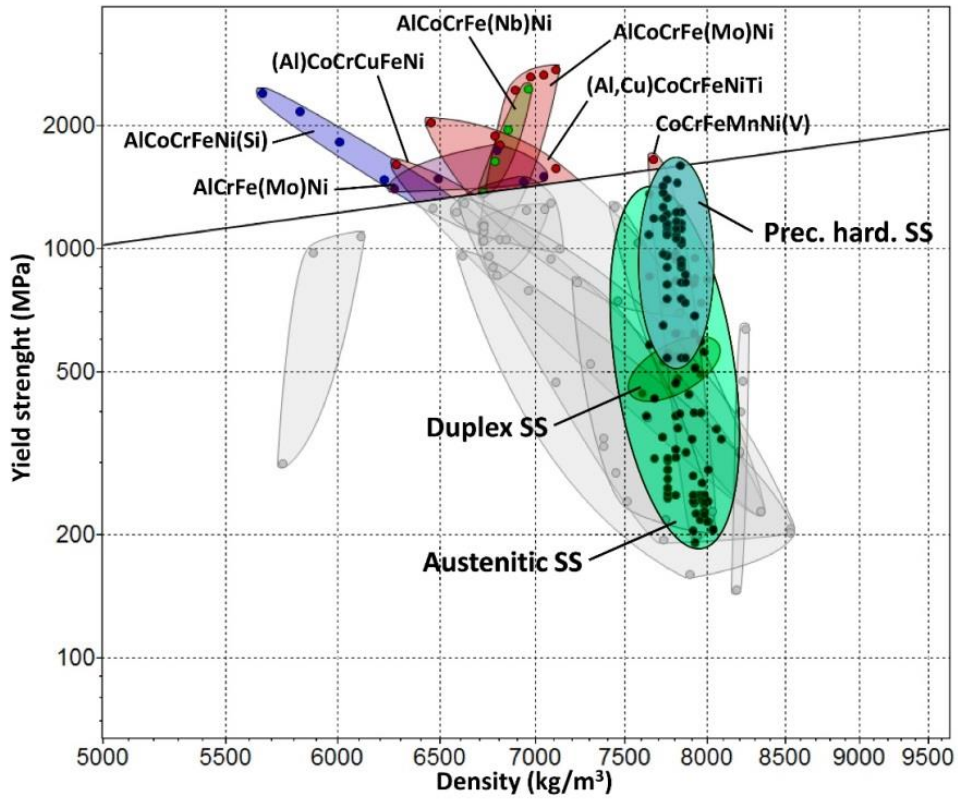


(b)

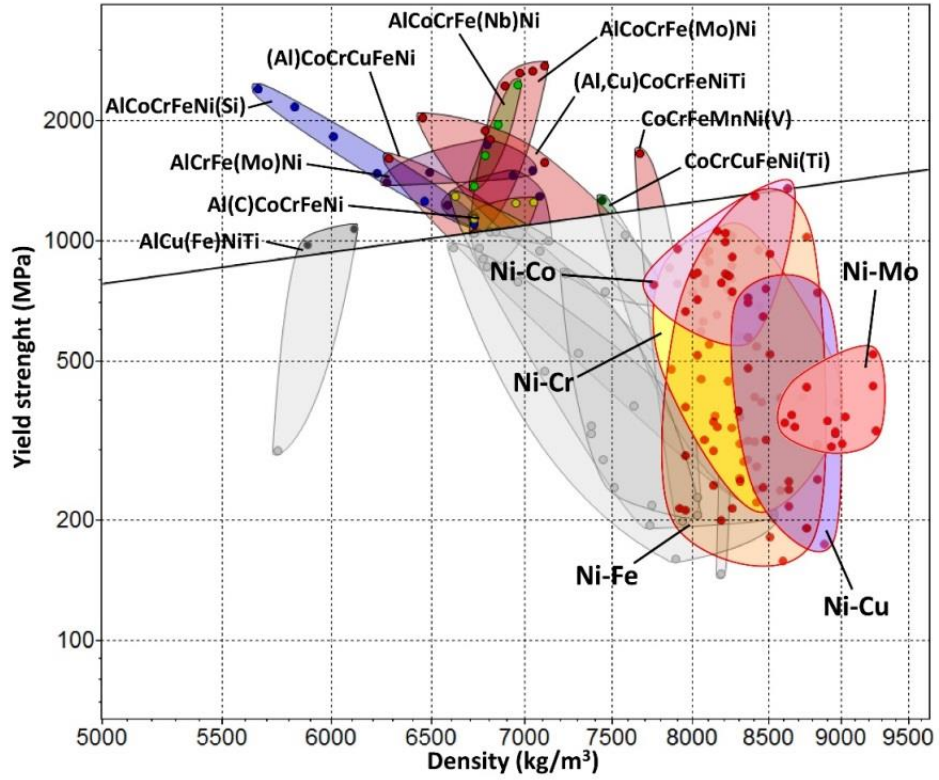
Figure 4: (a) Materials property space for room temperature Young's modulus vs density of conventional metal alloys and CCAs. 3d transition metal CCAs are shown by teal-colored bubbles and refractory metal CCAs are shown by yellow bubbles. The dashed lines give performance indices for uniaxial tension ( $s = 1$ ), beam bending ( $s = 2$ ) and panel bending ( $s = 3$ ). See the text for additional discussion of this plot. This chart was made with the CES EduPack database, Level 3 Aerospace edition and the CCA database from the present work. It displays data for about 1220 commercial and 115 multi-principle element alloys. (b) Room temperature yield strength plotted against Young's modulus for conventional metal alloys and CCAs. The contour (dashed line) shows the ratio of the yield strength over the Young's modulus.



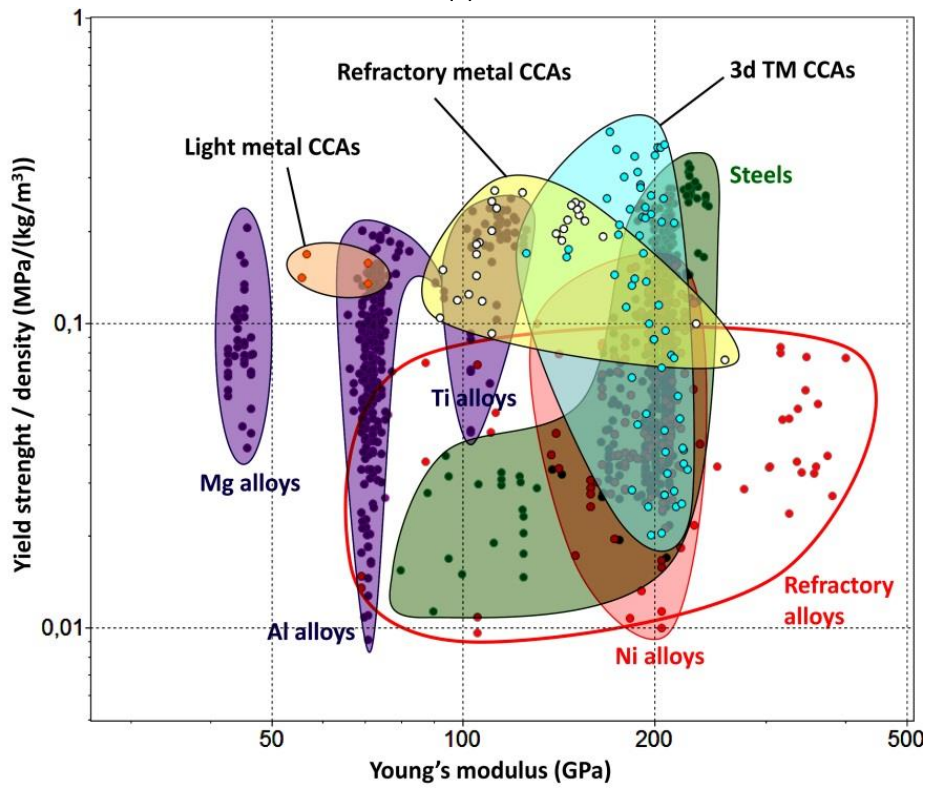
(a)



(b)



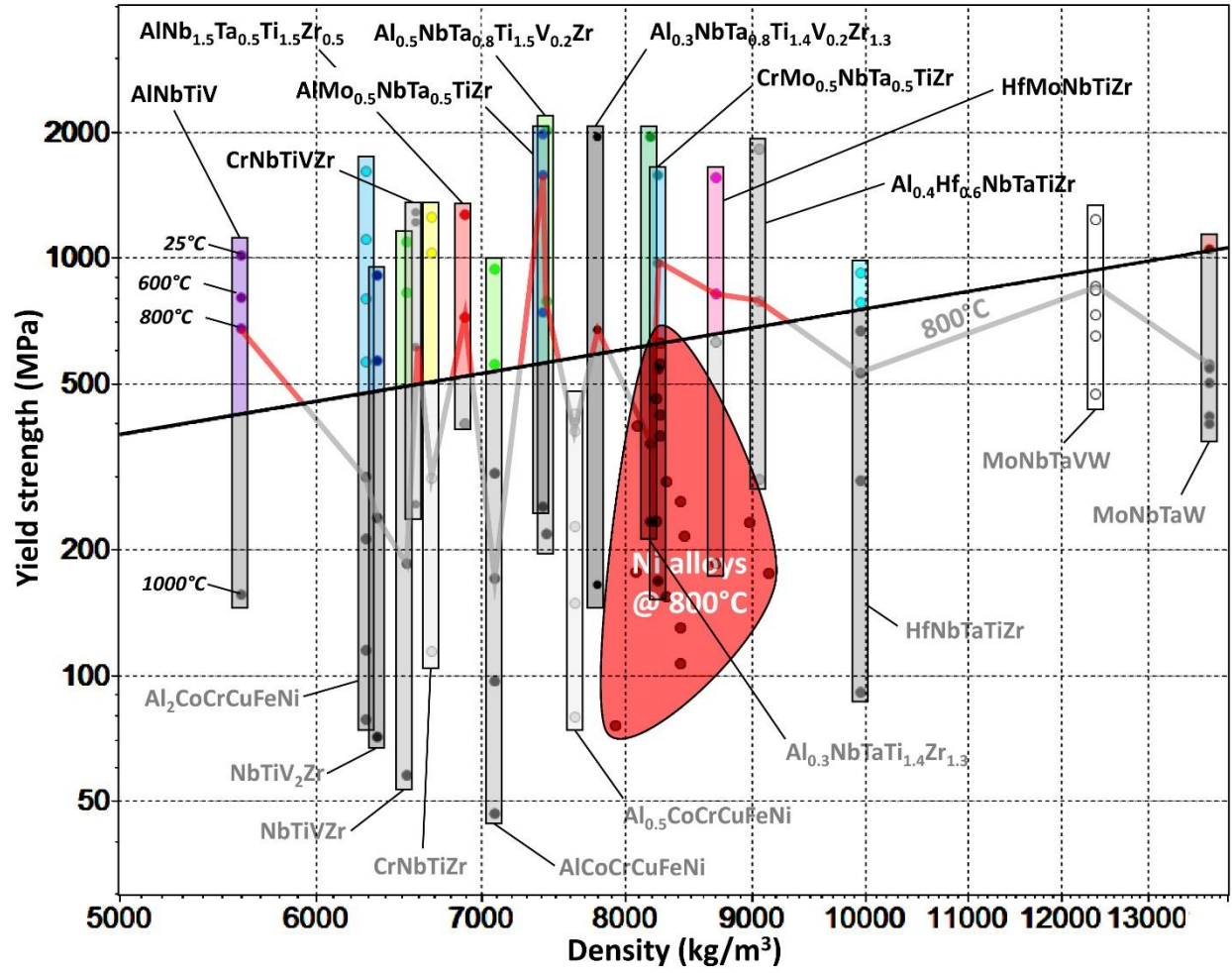
(c)



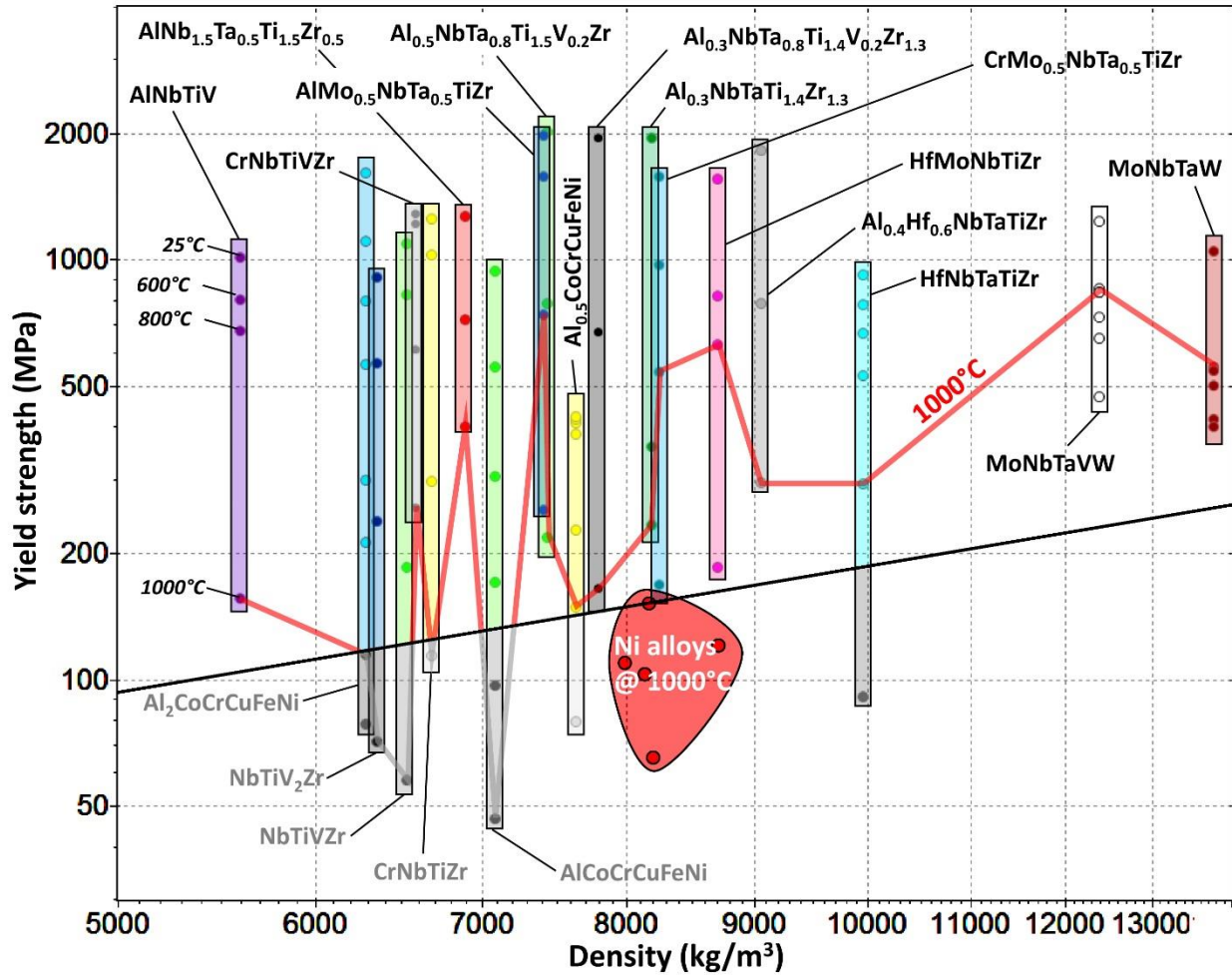
(d)

Figure 5: (a) Detailed illustration of 3d transition metal CCA alloy classes in room temperature yield strength vs density property space. 76 alloys are shown. (b) Comparison of 3d transition metal CCA alloy classes with three major classes of commercial stainless steels. Data for 136 stainless steel alloys are shown. (c) Comparison of 3d transition metal CCA alloy classes with selected classes of commercial Nickel alloys. Data for 119 Ni alloys are included. Individual alloys are shown by open and closed circles, and alloy classes are enclosed in bubbles. In (b,c), 3d transition metal CCAs above the performance index line for uniaxial tension (slope,  $s = 1$ ) are shown in color, whereas those below the line are shown in gray. This chart was made with the CES EduPack database, Level 3 Aerospace edition and the CCA database from the present work. (d) Specific Yield Strength versus Young's modulus for commercial alloys and different family CCAs.





(a)



(b)

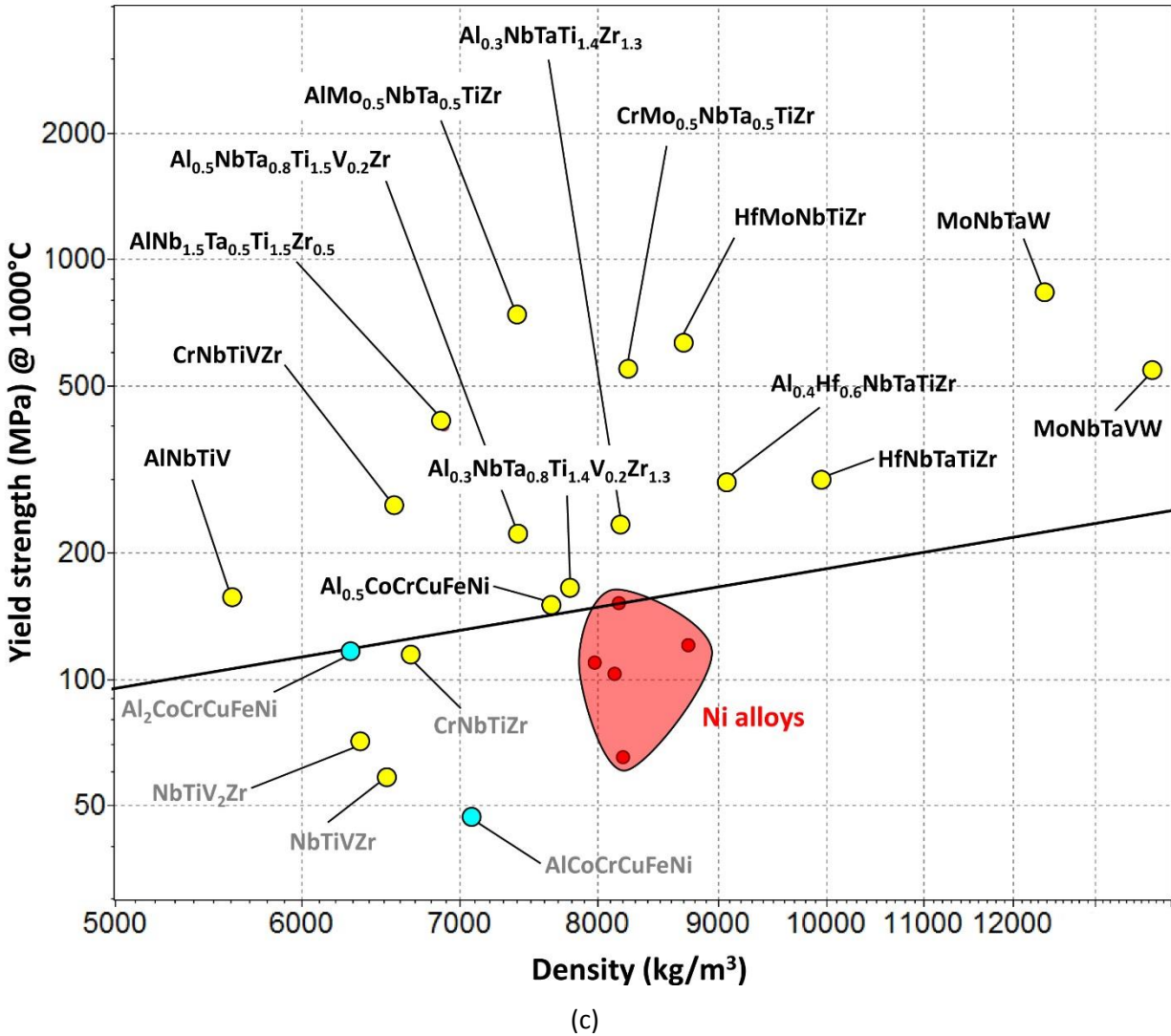
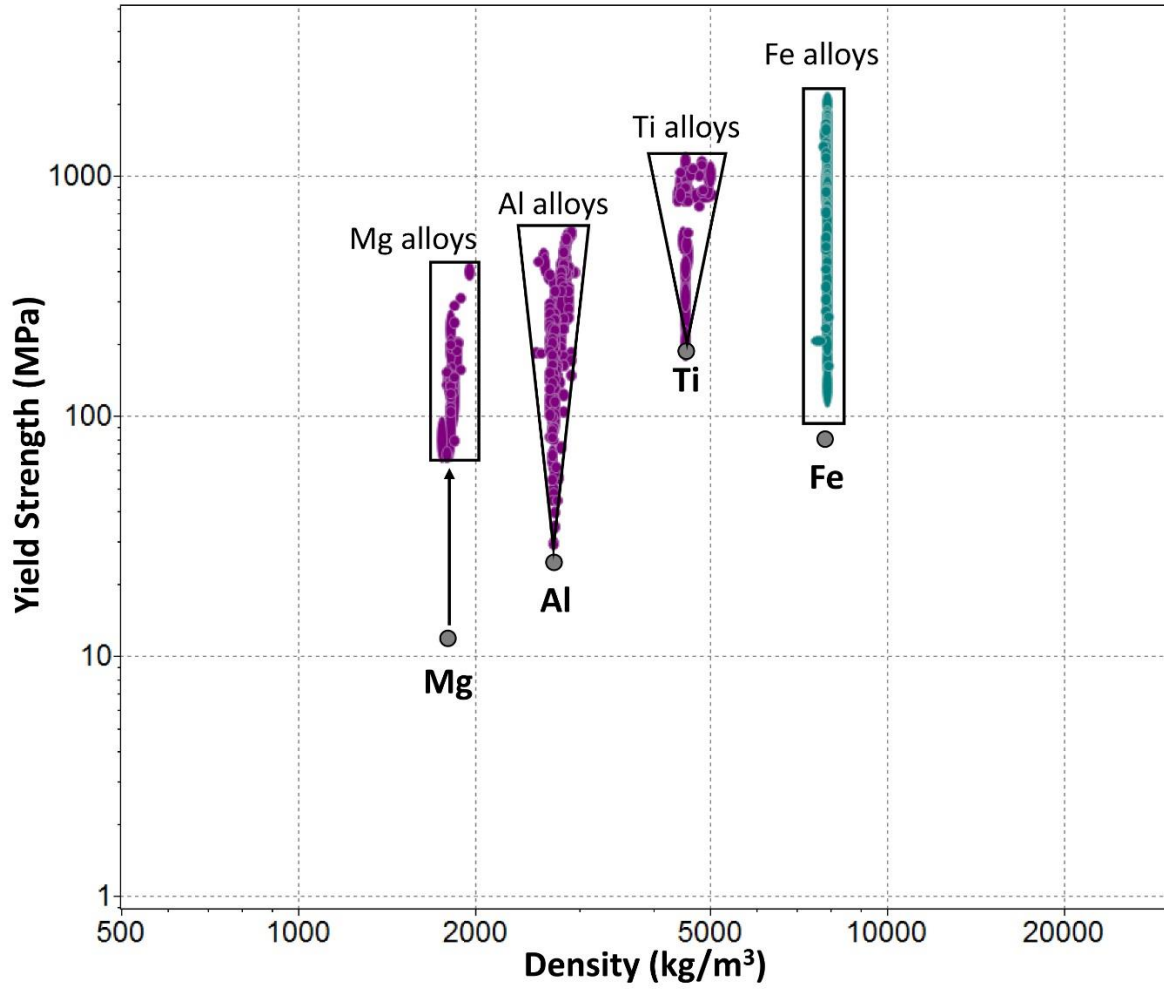
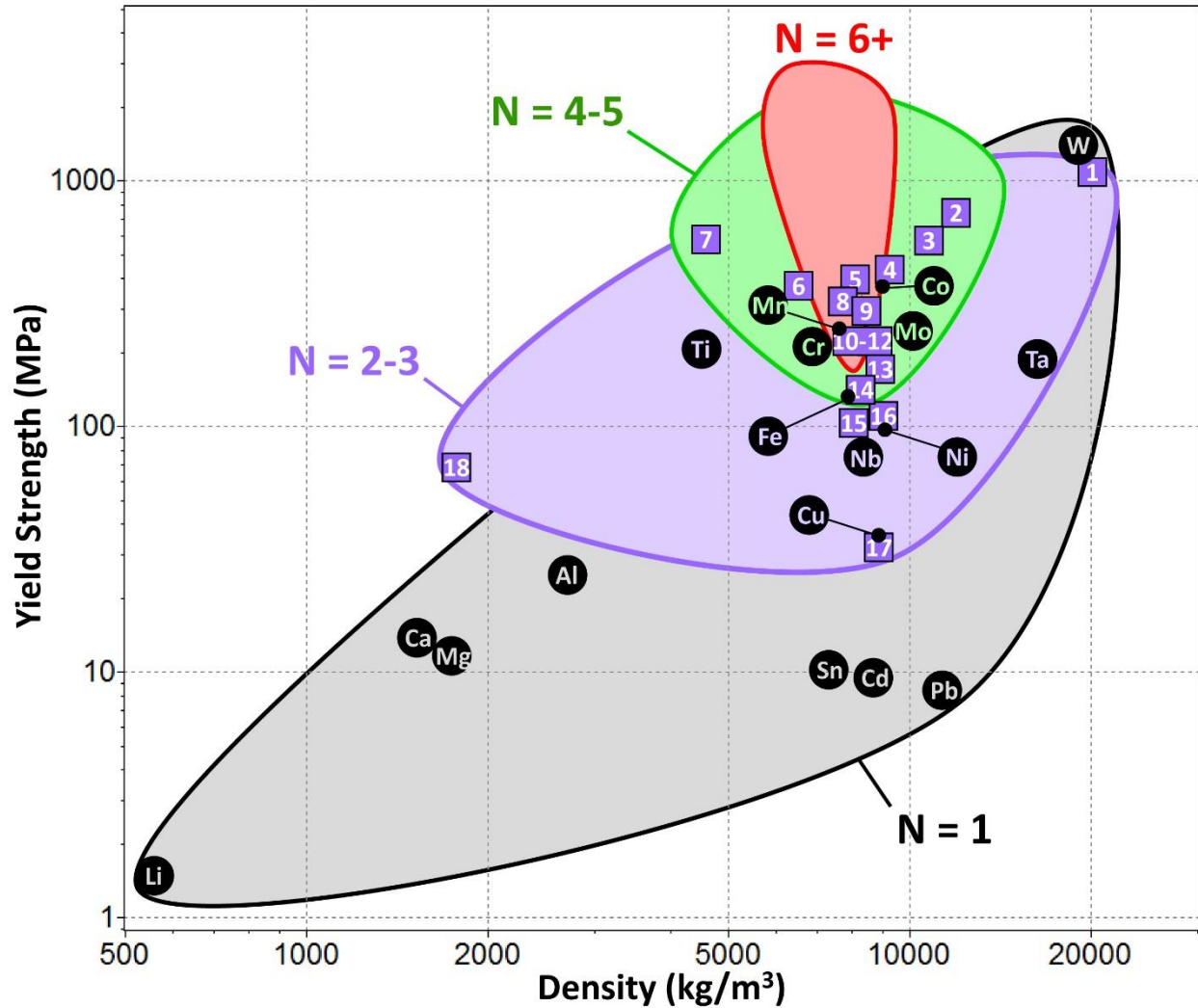


Figure 6: Materials property space for yield strength vs density as a function of the temperature. Individual CCAs are shown with vertical bars that provide alloy properties at a different temperatures. The red line connects yield strength values of CCAs at 800°C in (a) and 1000°C in (b). In (c) only the data at 1000°C are displayed. Data for 15 Nickel alloys at 800°C and 5 at 1000°C are shown for comparison, they include Ni-Cr Rene 41, Ni-Cr WASPALOY, Ni-Cr INCONEL 718, Ni-Cr INCONEL X-750, Ni-Cr INCONEL 706, Ni-Cr INCONEL 600, Ni-Cr INCONEL 625, Ni-Cr alloy INCONEL 754, Ni-Cr alloy HASTELLOY X, Ni-Co superalloy L605, Ni-Co superalloy HS 188, Ni-Fe alloy Haynes HR-110, and Ni-Fe superalloy N-155. CCA above the performance index line for uniaxial tension (slope,  $s = 1$ ) display their label above the line. This chart was made with the CES EduPack database, Level 3 Aerospace edition and the CCA database from the present work.

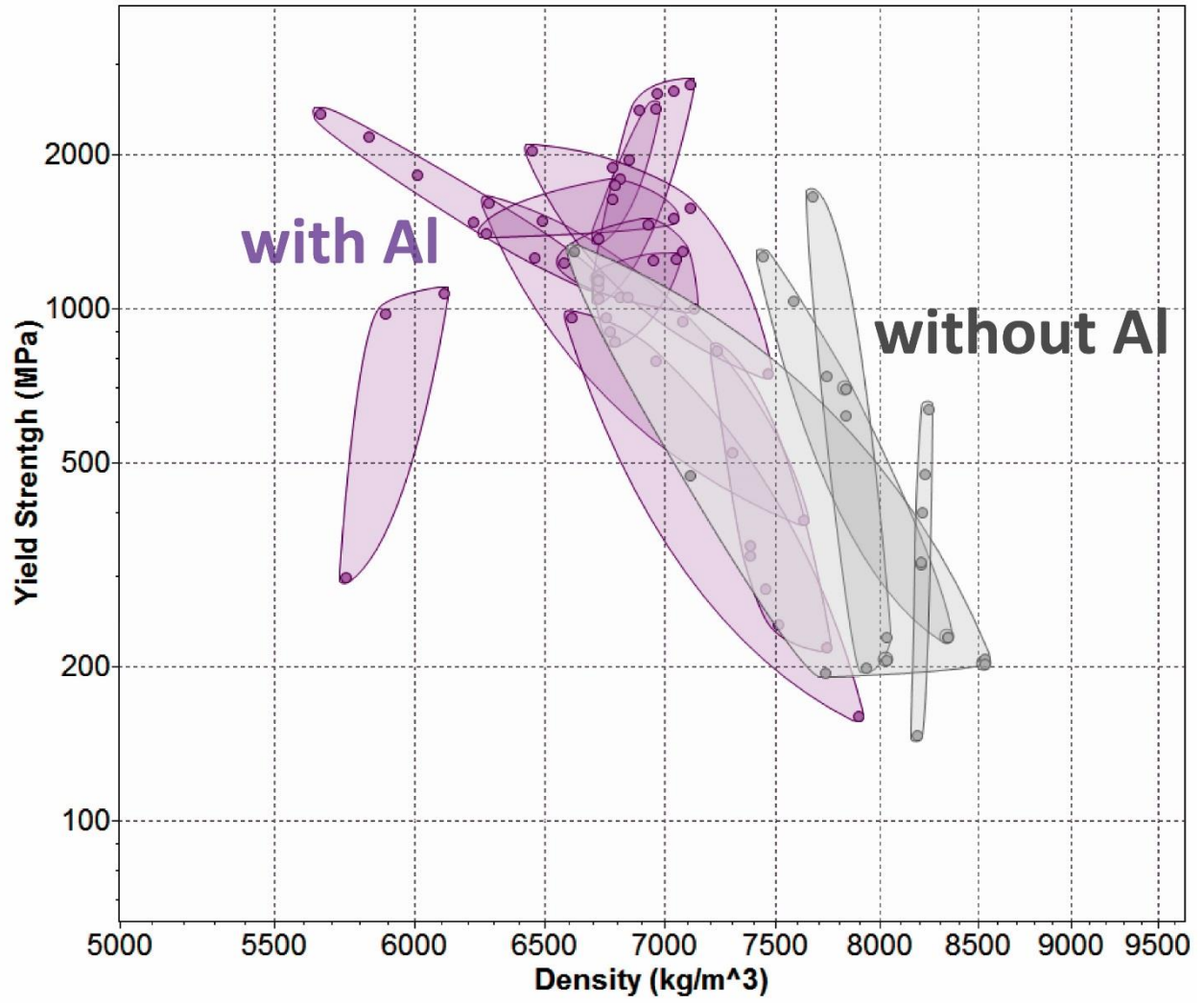


(a)

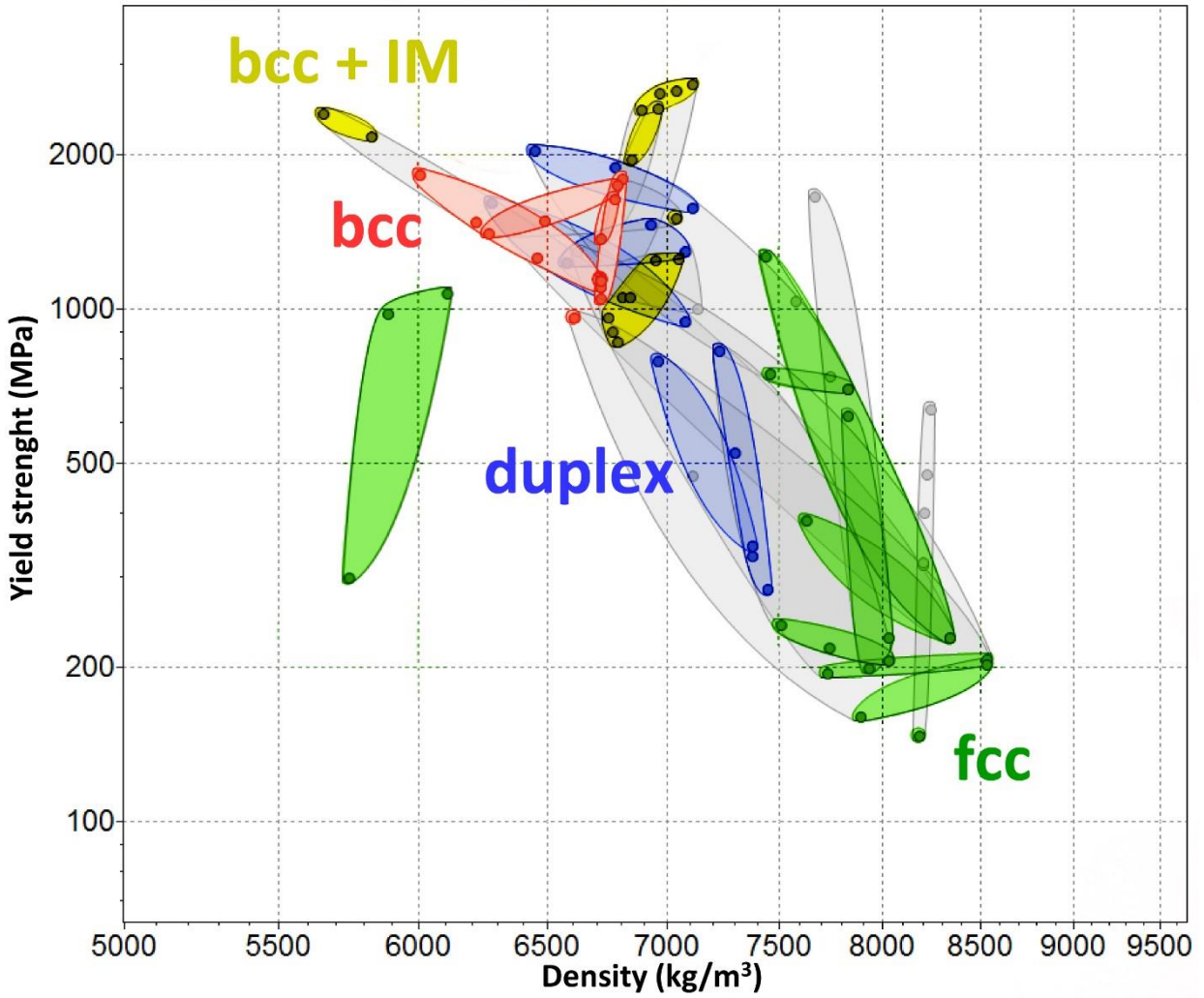


(b)

Figure 7: (a) The effect of alloying on room temperature specific yield strength for Al, Mg, Ti and Fe, and conventional alloys based on these elements. The alloy yield strengths are significantly higher than the base element, while the density changes are marginal. (b) The effect of alloying on room temperature specific yield strength for CCAs as a function of the number of principal elements. The range in densities shrinks while the yield strengths shift to higher values. The unary systems are labelled inside black circles. The binary and ternary systems are: (1) Re-W, (2) Mo-W, (3) Nb-Ta-W, (4) Mo-Ni, (5) Cr-Ni, (6) Ni-Ti, (7) Al-Nb-Ti, (8) Cr-Fe-Ni, (9) Co-Cr-Ni, (10) Fe-Ni, (11) Fe-Mn-Ni, (12) Co-Mn-Ni, (13) Co-Fe-Ni, (14) Cu-Ni, (15) Cu-Zn, (16) Co-Ni, (17) Pb-Sn, and (18) Li-Mg. The quaternaries and above use data from 3d TM CCAs, refractory CCAs, CCA bronzes and brasses, and light metal CCAs.

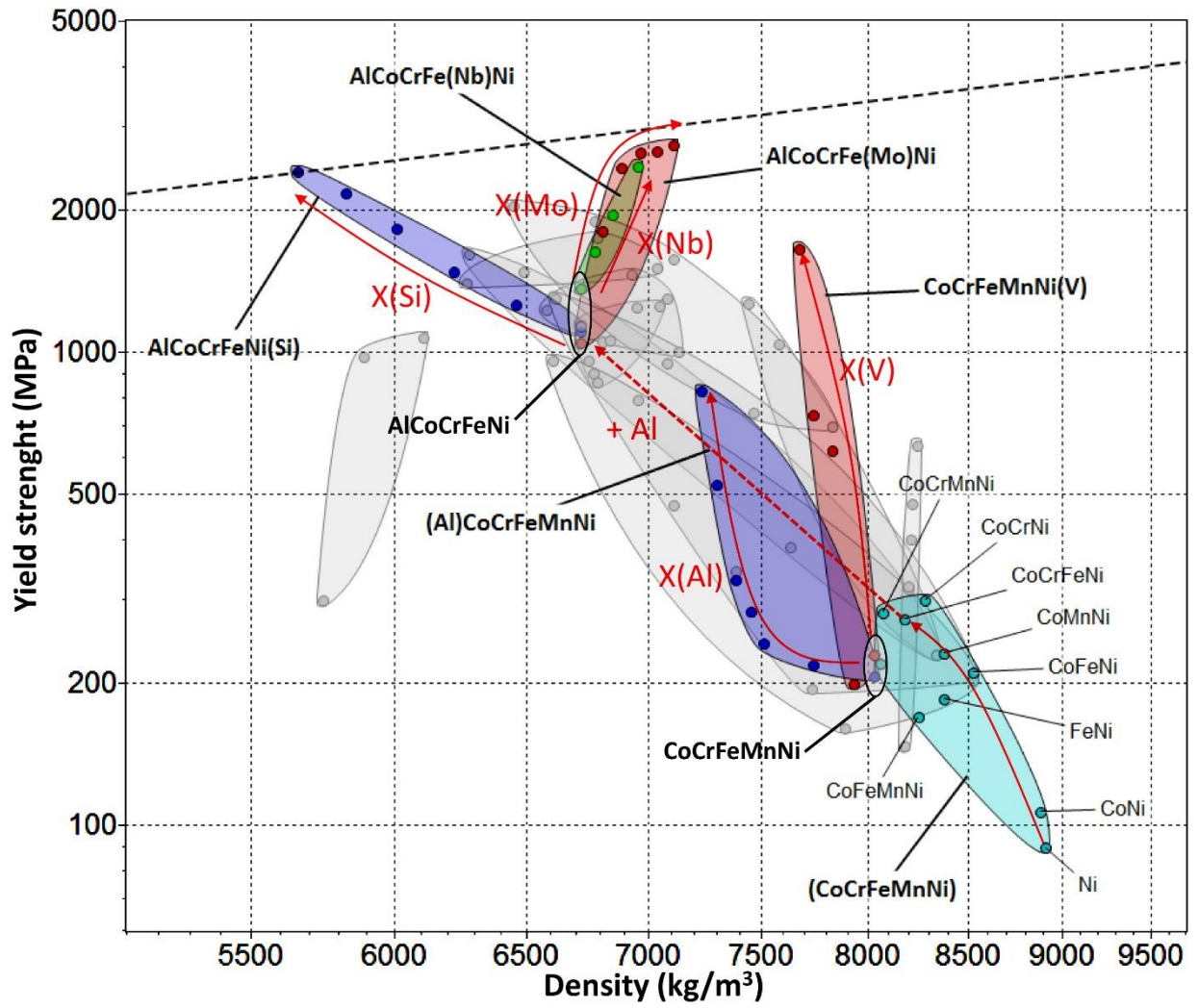


(a)



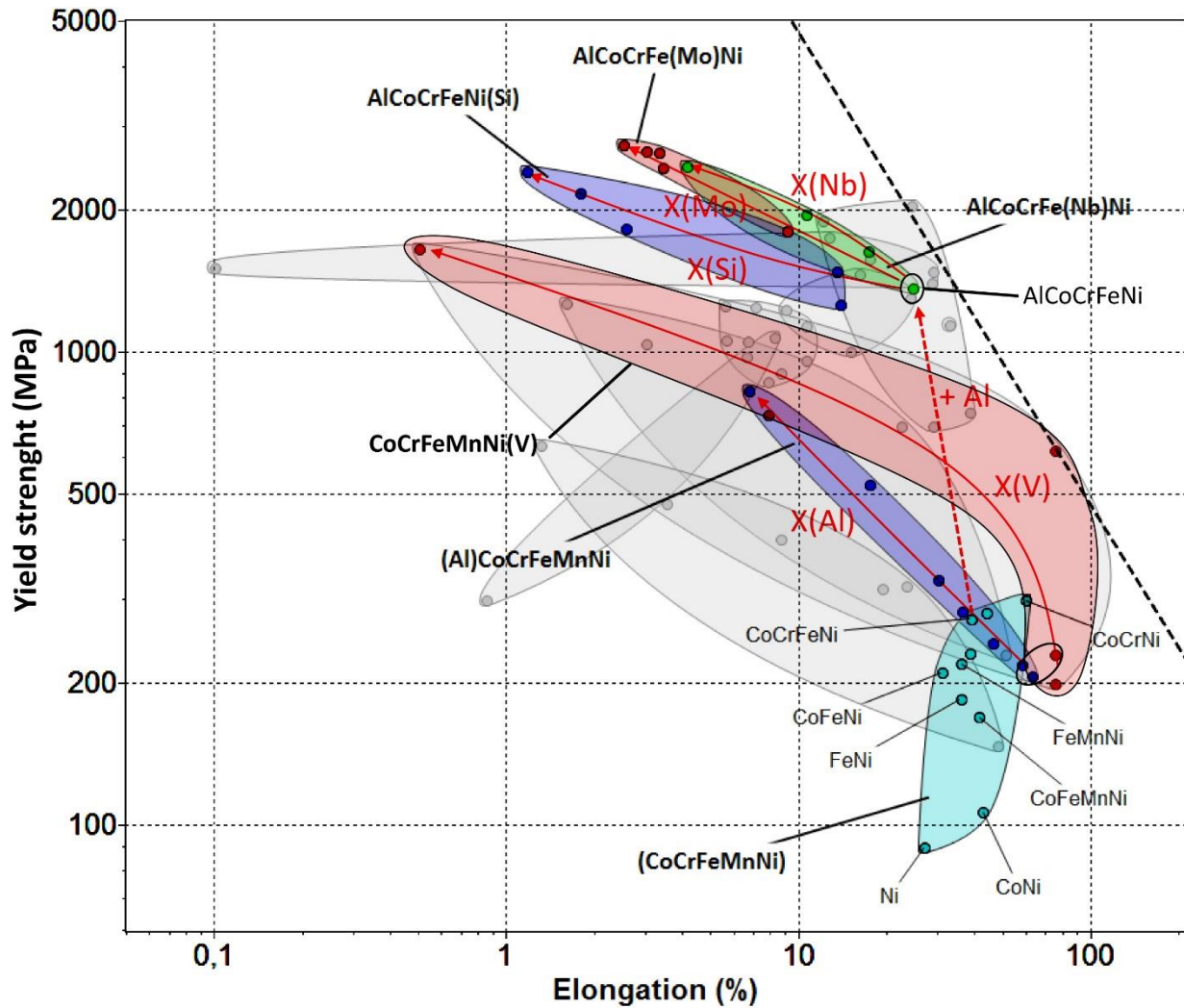
(b)

Figure 8: Materials property space for room temperature yield strength vs density showing the effect of Al addition on (a) the properties and (b) the resulting phases present for 3d TM CCAs.



(a)





(b)

Figure 9: Materials property space for (a) room temperature yield strength vs density and (b) room temperature yield strength vs elongation illustrating the influence of Al, Ni, V and Si on the properties of selected 3d TM CCAs. The dashed lines give performance indices for light component in uniaxial tension (slope,  $s = 1$ ) in (a), and the product of strength and ductility (slope,  $s = -1$ ) in (b).